



HAL
open science

Transcriptome profiling of gastric-type endocervical adenocarcinomas identifies key signaling pathways for tumor progression

Damien Vasseur, Jonathan Lopez, Sabrina Croce, Garance Tondeur, Lucie Bonin, Françoise Descotes, François Golfier, Mojgan Devouassoux-Shisheboran

► To cite this version:

Damien Vasseur, Jonathan Lopez, Sabrina Croce, Garance Tondeur, Lucie Bonin, et al.. Transcriptome profiling of gastric-type endocervical adenocarcinomas identifies key signaling pathways for tumor progression. *Gynecologic Oncology*, 2020, 157, pp.775 - 782. 10.1016/j.ygyno.2020.04.046 . hal-03490288

HAL Id: hal-03490288

<https://hal.science/hal-03490288>

Submitted on 9 Jun 2022

HAL is a multi-disciplinary open access archive for the deposit and dissemination of scientific research documents, whether they are published or not. The documents may come from teaching and research institutions in France or abroad, or from public or private research centers.

L'archive ouverte pluridisciplinaire **HAL**, est destinée au dépôt et à la diffusion de documents scientifiques de niveau recherche, publiés ou non, émanant des établissements d'enseignement et de recherche français ou étrangers, des laboratoires publics ou privés.



Distributed under a Creative Commons Attribution - NonCommercial 4.0 International License

Title Transcriptome profiling of gastric-type endocervical adenocarcinomas identifies key signaling pathways for tumor progression.

Short running title Gene-expression signature of gastric-type cervical carcinoma

Damien Vasseur^{1,3,*}, Jonathan Lopez^{1,2,3,*,§}, Sabrina Croce^{6,7}, Garance Tondeur⁵, Lucie Bonin⁴,
Françoise Descotes¹, François Golfier^{2,4}, Mojgan Devouassoux-Shisheboran^{2,3,7}

¹Hospices Civils de Lyon, Department of Biochemistry and Molecular Biology, Centre Hospitalier Lyon-Sud, France

² Université de Lyon, Université Claude Bernard Lyon 1, Lyon, France

³ Cancer Research Center of Lyon. INSERMU1052, Lyon, France

⁴Hospices Civils de Lyon, Department of Obstetrics and Gynecology, Centre Hospitalier Lyon-Sud, France

⁵ Hospices Civils de Lyon, Department of Pathology, Centre Hospitalier Lyon-Sud, France

⁶ Institut Bergonié, Department of Pathology, Bordeaux, France

⁷ Réseau INCa des tumeurs rares gynécologiques (TMRG) and GYNECO group (www.ovaire-rare.org/TMRG)

*These authors contributed equally to this work

§corresponding author

Correspondence: Dr Jonathan Lopez, Department of Biochemistry and Molecular Biology, Centre Hospitalier Lyon-Sud, Hospices Civils de Lyon, 165 Chemin du Grand Revoyet, 69310 Pierre-Bénite, France

E-mail: jonathan.lopez@chu-lyon.fr; Tel : +33 478861607

Conflict of interest: none declared

Abstract

Objective: Gastric-type endocervical carcinoma is a rare entity of carcinoma of the cervix. In contrast to the intestinal type, the gastric type is not related to Human Papilloma Virus (HPV) infection and has been reported to be much more aggressive than the usual type. Oncogenic pathways involved in this poor-prognosis phenotype are largely unexplored.

Methods: We compared activation of the main signaling pathways involved in cancer progression between the intestinal- (n=5), gastric- (n=6) and usual-type (n=6) adenocarcinomas of the cervix using a targeted transcriptomic approach (expression of 770 genes) on FFPE samples.

Results: We identified a gene-expression signature composed of 11 genes that allows the classification of these endocervical carcinoma as three distinct molecular entities. There were similarities between mucinous endocervical carcinomas (gastric and intestinal types) despite difference in pathogenesis related to HPV infection. Among HPV-related endocervical carcinoma, the intestinal type could be molecularly distinguished from the usual type by high expression of *EIF2AK3* and low expression of *PPFIBP2* genes, supporting its classification as a distinct entity. Overexpression of *TAL1* and *S1PR1* genes were characteristic of the gastric type. The usual type was characterized by high expression of occludin and *VAV3* genes. Tight junction disruptions might play an essential role in the metastatic potential of mucinous endocervical carcinoma with concomitant loss of OCLN and claudin 4 proteins. An overexpression of *NTRK1* transcript was observed in mucinous endocervical carcinomas when compared to the usual type.

Conclusions: This transcriptomic study identified a signature that supports the classification of endocervical carcinomas as three distinct entities: usual-, intestinal- and gastric-type. It

also points out to disruption of tight junctions as a potential mechanism of metastatic dissemination of these rare tumors.

1. Introduction

First described by Kojima et al. in 2007[1], endocervical adenocarcinoma of gastric-type (G-ECA) has been introduced into the 2014 edition of the World Health Organization (WHO) classification under the category of mucinous endocervical adenocarcinomas [2]. This category also includes intestinal-type adenocarcinoma (I-ECA) and signet ring cell adenocarcinoma. The intestinal-type is a mucin-producing adenocarcinoma showing tumor glands lined by goblet cells. Gastric-type account for 20% of all endocervical adenocarcinomas in Japan [1], and 10% in an international population [3]. This entity is characterized by tumor glands resembling gastric and pyloric epithelium with gastric-type mucin and expression of MUC6 in 31 [1] to 80% [5] of cases.

Although gastric-type and intestinal-type endocervical adenocarcinomas are both mucin-producing adenocarcinomas and grouped under the same category in 2014 WHO classification, they differ in their pathogenesis. Indeed, the intestinal-type is related to Human Papilloma Virus (HPV) infection and is associated with adenocarcinoma in situ similar to the usual type endocervical adenocarcinoma (U-ECA), while the gastric-type is usually not related to HPV. Adenocarcinoma in situ is rarely considered as its precursor, which seems to be more often lobular endocervical gland hyperplasia [6]. Since G-ECA are not associated with HPV infection, p16 is rarely expressed while p53-mutated type immunostaining is seen in 41% of cases [5]. Besides, some patients with G-ECA have been reported with Peutz-Jeghers syndrome, and somatic serine-threonine kinase (*STK11*) gene mutation is detected in half of the sporadic cases [7]. The underlying molecular pathways altered in the gastric-type are not very well known. Recently, a massively-parallel sequencing molecular study has been reported on 14 cases of G-ECA [8], showing genetic heterogeneity in these tumors. *TP53* was the most recurrently mutated gene followed by

mutS homolog 6 (*MSH6*), cyclin-dependent kinase inhibitor 2A (*CDKN2A/B*), DNA polymerase epsilon (*POLE*), SLX4 structure-specific endonuclease subunit (*SLX4*), AT-rich interaction domain 1A (*ARID1A*), *STK11*, BRCA 2 DNA repair associated (*BRCA2*) and mutS homolog 2 (*MSH2*). An amplification in MDM2 proto-oncogene (*MDM2*) gene was reported in two cases without *TP53* mutation.

To better investigate the molecular pathogenesis and the metastatic potential of mucinous endocervical adenocarcinoma, including gastric- and intestinal-type ECA, we undertook a molecular study using targeted transcriptomic profiling of a series of these tumors in comparison to usual type endocervical adenocarcinomas (U-ECA).

2. Methods

2.1. Patient's selection: This is a retrospective study of all recorded cases of endocervical adenocarcinomas between January 2005 and May 2016 at Lyon University Hospital, Hospices Civils de Lyon (Hôtel Dieu, Croix Rousse and Lyon Sud). All HES (Hematoxylin, Eosin, Saffron) slides of 82 cases were reviewed independently by two pathologists (MDS and SC). Among these cases, only 18 met the criteria for mucinous adenocarcinomas (10 G-ECA and 6 I-ECA). We excluded from the study mucinous signet ring cell adenocarcinomas because of the low number (n=2). One case of intestinal-type had scarce tissue material for analysis. Six cases of usual type endocervical adenocarcinomas (U-ECA) were also retrieved from the files and used as controls. For each case, a representative formalin-fixed, paraffin-embedded (FFPE) tissue block was selected for the immunohistochemical and molecular studies.

2.2. Immunohistochemistry and in situ hybridization (ISH): The study was performed on Ventana Benchmark automated immunostainers with the following antibodies: p16 (clone

E6H4, Ventana-Roche, prediluted), p53 (clone DO-7, Ventana-Roche, prediluted), MUC6 (clone CLH5, Leica, prediluted), claudin 4 (EPRR17575, Abcam, 1/500) occludin (OCLN) (clone OC-3F10, Invitrogen, 1/100) and TRKpan (clone A7H6R, 92991 S, Ozyme, Cell Signaling, 1/50).

p16 staining was considered as positive if the stain was nuclear and cytoplasmic and continuous and diffuse. p53 staining was considered as mutated-type if > 80% of nuclei were stained strongly or if negative [9,10]. MUC6 stain was cytoplasmic.

An immunostaining score was performed for CLDN4 and OCLN by multiplying the percentage of the stained cells by the intensity of staining (1, 2, 3).

We performed ISH to detect HPV DNA using a biotinylated DNA probe set (Kit ISH Iview Blue Plus, Ventana-Roche) according to the manufacturer's protocols. Nuclear dot signals were considered positive.

2.3. NanoString analysis: RNAs were extracted from FFPE tumors. Depending on the size of each lesion between two and six 5- μ m slides were used. Slides were first dewaxed with two baths of D-Limonene (2min) and a bath of Absolut Ethanol (2min). RNA extraction was then performed using High Pure FFPE RNA Isolation Kit (Roche, Switzerland, #06483852001). Depending on concentrations, hybridization with Human PanCancer Progression probes (Nanostring Technologies, USA, #XT-CSO-PROG1-12) was performed using 88 ng to 175ng RNA, according to manufacturer instructions. This panel targets 770 mRNA involved in cancer progression, invasion and metastases plus 30 housekeeping genes for normalization. After 19 hours of incubation at 65°C, samples were processed on a Nanostring nCounter FLEX platform. Raw counts for individual digital molecular barcodes were normalized on six positive internal controls and thirty housekeeping genes using nSolver 4.0 analysis software

(Nanostring Technologies, USA). The background was estimated from blank wells and six negative internal controls and removed from raw counts.

2.4. Statistical Analysis: Expression of the 770 genes was compared between gastric-, intestinal- and usual-type ECA. For each gene, a fold change ratio and FDR-adjusted p-value were computed. To visualize the differences observed between our two populations, we used R Studio software (v1.1.463) and generated heatmaps, Principal Component Analysis (PCA) and correlogram. Heatmaps were built using heatmap.3 from gplots 3.0.0 R package. PCA and biplot were obtained using factomineR 1.41 and factoextra 1.0.5 R packages, respectively. Keeping two components for PCA explained 70.3% of the total variance (55.6% for PC1 and 14.7% for PC2). Correlogram resulted from a Pearson test with an alpha=0.05 and was realized using corrplot 0.84 R package. Network analysis was performed using STRING database (<https://string-db.org/>). Finally, Welch two-sample test used to compare the level of expression of OCLN and CLDN4 was performed using the t-test function on R.

3. Results

3.1. Clinical presentation, histopathology and immunostainings

The immunohistochemical study was performed on 22 ECA, organized into three groups of G-ECA, I-ECA and U-ECA.

Ten cases showed the characteristic morphology of gastric-type adenocarcinomas [4]. Eight tumors were composed of glands of various sizes, occasionally presenting intraluminal papillae, lined by very large cells with distinct cell borders and clear or pale cytoplasm, sometimes with foamy or densely eosinophilic cytoplasm (Figure 1A). Two cases showed the morphology of minimal deviation adenocarcinoma, which is a very well-differentiated variant of G-ECA, with large and cystic glands infiltrating the cervical stroma. The nuclei

were very bland in the well-differentiated variant while they showed atypia with prominent nucleoli in the six classic G-ECA. On immunohistochemical study, all but four cases of classic G-ECA were positively stained with MUC6. These four MUC6 negative cases were excluded from the study. Only cases with no doubt on the gastric-type differentiation were included in the molecular analyses (n = 6). All the 6 cases of G-ECA were P16 and HPV negative. One case showed a mutated p53 immune profile. In this group, patients' age ranged from 32 to 51, with a mean of 42.3 years. The FIGO stage at diagnosis was IB in 4 and IIA in 2 cases.

Five cases showed the characteristic morphology of I-ECA. They were composed of tumor glands entirely lined by mucin-producing goblet cells (Figure 1B). In three cases, a colloid pattern was seen with pools of mucin dissecting the cervical stroma, associated with intestinal-type malignant glands. All cases of I-ECA were p16 and HPV positive and showed a wild-type immune profile for p53. Three cases stained for MUC6. In this group, patients' age ranged from 29 to 70, with a mean of 43 years. The FIGO stage at diagnosis was IB in 4 and IA2 in one case.

Six cases of U-ECA showed a well-differentiated proliferation of glands lined by stratified columnar cells with no or very little endocervical type mucin, showing many mitoses and apoptotic bodies (Figure 1C). All these cases were p16 and HPV positive, MUC6 negative and showed a wild-type immune profile for p53. In this group, patients' age ranged from 34 to 62, with a mean of 44.5 years. The FIGO stage at diagnosis was IB in 5 cases and IA2 in the last case.

3.2. Differentially-expressed genes between mucinous and usual-type ECA

First, we compared mucinous (G-ECA plus I-ECA groups) versus usual type adenocarcinomas (U-ECA) to identify candidate genes capable of discriminating these two entities. Differentially-expressed genes were ranked on False Discovery Rate (FDR)-adjusted p-

values. Setting up the FDR cut-off at 0.2, we retained nine candidate genes: neurotrophic receptor tyrosine kinase 1 (*NTRK1*), KiSS-1 metastasis suppressor (*KISS1*), somatostatin receptor 2 (*SSTR2*), occludin (*OCLN*), sphingosine-1-phosphate receptor 1 (*S1PR1*), TAL bHLH transcription factor 1 (*TAL1*), thromboxane A2 receptor (*TBXA2R*), thrombospondin 4 (*THBS4*) and vav guanine nucleotide exchange factor 3 (*VAV3*). Most of the genes were less expressed in the usual type compared to mucinous endocervical carcinomas except for *OCLN* and *VAV3* with fold changes of +2.6 and +5.7, respectively (Supplementary Table 1). Hierarchical clustering heatmap confirmed the robustness of this nine-genes signature to discriminate the mucinous from U-ECA (Figure 2A). The distance matrix representation (Figure 2B) objectifies that U-ECA cases form a homogeneous group wide-different from mucinous ECA. As expected, it also emphasizes that mucinous carcinoma is a more heterogeneous entity at the molecular level.

One of the most discriminant gene between mucinous (G-ECA plus I-ECA groups) and U-ECA was *OCLN*. This gene encodes a membrane protein localized in tight junctions. The level of expression of this gene (Nanostring counts) was statistically decreased in mucinous ECA when compared to the U-ECA ($p=0.001$ at 95% CI). We confirmed the loss of *OCLN* at the protein level by immunohistochemistry ($p=0.005$ at 95% CI). Importantly, levels of *CLDN4*, another essential protein of the tight junction, were also significantly decreased in both gastric and intestinal types ($p\text{-value}=0.036$ at a risk $\alpha=5\%$) (Figure 3). These results point out to tight junctions' disruptions as a potential mechanism explaining the aggressive phenotype of these rare tumors.

3.3. Comparison of genes expression between gastric-type and intestinal-type ECA

To further explore the phenotypic heterogeneity of mucinous ECA, we compared genes expression profiles between G-ECA and I-ECA. Using the same filtering strategy, we

identified 11 differentially-expressed genes (Supplementary Table 2) able to segregate these two mucinous subtypes. Heatmap of these genes demonstrated a clear clustering of I-ECA and G-ECA (Figure 4A). Compared to the intestinal type, the gastric type ECA presented with high levels of PPFIA binding protein 2 (*PPFIBP2*), DENN domain-containing 5A (*DENND5A*), asporin (*ASPN*), GATA binding protein 4 (*GATA4*), vascular endothelial growth factor B (*VEGFB*) and zinc finger FYVE-type containing 16 (*ZFYVE16*). On the other hand, the intestinal-type endocervical carcinomas presented high expression of heat shock protein 90 beta family member 1 (*HSP90B1*), AKT serine/threonine kinase 1 (*AKT1*), ribosomal protein S6 kinase B2 (*RPS6KB2*), eukaryotic translation initiation factor 2 alpha kinase 3 (*EIF2AK3*) and PTTG1 regulator of sister chromatid separation (*PTTG1*) (Figure 4A). Using the STRING database to test functional protein association networks, we identified a strong implication of the AKT pathway in differentiating gastric from intestinal types with six out of the eleven differentially-expressed genes included in this pathway: *HSP90B1*, *AKT1*, *RPS6KB2* and *EIF2AK3* high in I-ECA versus *GATA4* and *VEGFB* high in G-ECA (Figure 4B). Altogether, these results emphasized that gastric- and intestinal-type ECA activate distinct signaling pathways.

3.4. Comparison of HPV-related and gastric-type endocervical adenocarcinomas

When comparing gastric-type with HPV related endocervical adenocarcinomas (intestinal and usual types), two discriminant genes were identified: RB transcriptional corepressor like 1 (*RBL1*) (FDR=0.02) and *CDKN2A* (FDR=0.09). We then built up a composite a gene-expression signature capable of classifying these three entities. We associated the nine genes of the first signature segregating mucinous from U-ECA to the two most discriminant genes of the I-ECA versus G-ECA signature. We obtained an 11-gene signature based on the expression of *EIF2AK3* (high in I-ECA), *PPFIBP2* (high in G-ECA compared to I-ECA), *NTRK1*,

KISS1, *SSTR2*, *TAL1*, *S1PR1*, *TBXA2R*, *THBS4* (low in U-ECA) and *OCLN* and *VAV3* (high in U-ECA). This composite signature was able to cluster the three subtypes (Figure 5A) efficiently. Next, we performed a PCA using two dimensions (Figure 5B). The first dimension which explains 55.6% of the total variance, opposes all U-ECA samples plus I3 with high levels of expression of *VAV3*, *OCLN* and *PPFIBP2* to mucinous ECA with high levels of expression of the others genes (most contributory: *SSTR2*, *NTRK1*, *S1PR1*, *KISS1* and *TAL1*). Higher expression of neurotrophic receptor tyrosine kinase 1 (*NTRK1*) transcript was observed in both intestinal- and gastric-type endocervical adenocarcinomas. The second dimension explained 14.7% of the total variance. It allowed distinguishing the intestinal type with high expression of *TBXA2R* and *EIF2AK3* from the gastric type of carcinomas of the cervix. The most contributory genes overexpressed in G-ECA were *PPFIBP2* and *TAL1*.

The matrix correlogram (Figure 6) confirmed the positive correlation between *VAV3* and *OCLN* (high in the usual type, $r^2= 0.84$) and the negative correlation of these two genes with all the others. In mucinous endocervical adenocarcinomas, the two pairs of overexpressed genes most positively correlated were: *NTRK1/SSTR2* and *TAL1/SSTR2* ($r^2=0.83$ and 0.81 respectively).

Discussion

Here we describe a gene-expression signature composed of 11 genes which allows the distinction between the three most frequent type of ECA, usual type, gastric-type and intestinal-type (Figure 5). Given the small size of this cohort due to the rarity of these tumors, this set of genes needs to be further validated in an independent cohort. Nevertheless, this study points out to relevant biological functions that might explain the

differential metastatic potential of these three entities and provide new therapeutic opportunities.

The mucinous adenocarcinoma of the cervix comprises two different subtypes of carcinomas with distinct biology and behavior. Indeed, G-ECA is a non-HPV-related carcinoma with important differences in tumor behavior and patient survival. Patients with G-ECA have a significantly worse clinical outcome, even when matched for stage and G-ECA more frequently metastasize to distant sites, including viscera and peritoneum when compared to usual-type adenocarcinoma [11]. However, I-ECA lumped together with the G-ECA under the same category by 2014 WHO classification, have a histogenesis and clinical behavior closer to usual-type ECA than G-ECA. Indeed, I-ECA is HPV-related and has the same prognosis as the usual-type adenocarcinoma when matched for the stage. A new international classification of endocervical adenocarcinoma recommends to classify uterine cervical carcinomas in two categories of HPV-associated (usual or mucinous, essentially intestinal) and HPV unassociated (gastric, clear cell, endometrioid, mesonephric) carcinomas [3]. Indeed, when comparing HPV-dependent ECA (I-ECA and U-ECA) with non-HPV-related ECA (G-ECA) in our series, two discriminant genes were identified, *RBL1* and *CDKN2A*. These two cell cycle regulators have already been found to be more expressed in HPV-positive oropharyngeal squamous cell carcinomas compared to the HPV-negative forms [12]. However, our study also shows that intestinal-type ECA has a distinct molecular signature that differs from U-ECA.

We report a significant increase of expression of *NTRK1* transcript in both intestinal and gastric types ECA when compared to the usual type (Figures 2 & 5, Supplementary Table 1). *NTRK1* is a receptor for the nerve growth factor and is overexpressed in lung [13], thyroid [14] and many other cancers, mainly by gene fusion mechanisms. However, we were not

able to detect any NTRK1 fusion in our samples nor to objectify its overexpression at the protein level using a panTRK antibody. This discrepancy between RNA and protein might be explained by a lack of sensitivity of the immunohistochemical staining due to: 1/ a weak level of basal expression in U-ECA (RNA counts $22,26 \pm 2,84$ compared to $370,62 \pm 96,53$ for *OCLN*) and 2/ a fold-change of 1.85 between the 2 groups (but highly significant with an FDR-adjusted p-value of 0.04). Additional studies are needed on a more significant number of mucinous ECA to confirm this finding.

Intestinal- and gastric-type ECA are sharing common transcriptomic patterns that allow to distinguish them from the usual-type ECA (Figure 2). Among them, the loss of occludin and claudin 4 (Figure 3) that lead to tight junctions disruptions may explain the difference in their metastatic potential. Loss of *OCLN* in breast cancer has been associated with modification of the membrane permeability and metastatic disease [15]. Reduced expression of *OCLN* by hypermethylation of its promoter also decrease sensitivity to apoptotic cell death [16].

Other genes involved in cell adhesion and metastatic dissemination pathways were also altered. *THBS4*, another protein involved in cell-cell adhesion and the remodeling of the extracellular matrix, was overexpressed in mucinous compared to usual-type ECA. Importantly *THBS4* gene was reported to facilitate invasion and dissemination of tumor cells in gastric [17], colorectal [18], prostate [19] and breast cancer [20]. We also observed an increase of *S1PR1* gene expression in mucinous carcinomas (I-ECA and G-ECA). *S1PR1* has been identified as a target to inhibit signal transducer and activator of transcription 3 (*STAT3*) signaling in DLBCL [21]. After secretion of S1P by tumor cells, the S1P-S1PR1 complex promotes resistance to apoptosis, cell proliferation and migration and increased resistance to treatment [22]. This receptor is also implicated in the tumor

neovascularization [23]. High levels of *S1PR1* are therefore associated with a more aggressive disease with a higher risk of metastases. *TBXA2R* gene encodes a G protein-coupled receptor. The oncogenic role of this receptor has been well described. *TBXA2R* gene was reported to increase tumor cell migration in prostate cancer [24], to reduce disease-free survival in breast cancer [25] and to increase cell proliferation in lung cancer [26]. Here we describe a significantly higher *TBXA2R* gene expression in intestinal- and gastric-type compared to usual-type ECA. *KISS1* gene is another interesting player in cancer. It encodes a ligand of a G protein-coupled receptor called GPR54. *KISS1* has been initially described as a tumor suppressor and anti-metastatic gene in numerous cancers such as melanoma [27], bladder [28], breast [29] and lung cancers [30]. Surprisingly, we observed higher levels of *KISS1* in mucinous carcinomas as compared to U-ECA. Similar results were reported in breast [31] and thyroid [32] cancers with significantly higher expression of *KISS1* in patients with aggressive tumors and dissemination potential. Thus, *KISS1* seems to play a dual role in cancer development. There was also a significant difference in the expression of *TAL1*, *VAV3* and *SSTR2* in U-ECA and mucinous intestinal and gastric type carcinomas. *VAV3* is underexpressed in mucinous carcinomas whereas *TAL1* and *SSTR2* are overexpressed in these tumors when compared to usual type U-ECA. However, the biological significance of these three genes has to be further explored.

Altogether, these findings show that at the molecular level, I-ECA differs from U-ECA and shares molecular similarities with G-ECA. Indeed, loss of *OCN* and *VAV3* and increased expression of *TAL1*, *SSTR2*, *THBS4*, *S1PR1*, *TBXA2R* and *KISS1* are molecular characteristics of mucinous carcinomas, of intestinal and gastric type and may explain in part their metastatic potential.

If intestinal and gastric types share some common signaling pathways, they are also distinguishable based on the expression of two genes: *EIF2AK3* and *PPFIBP2*. *EIF2AK3* is increased in I-ECA compared to G-ECA and U-ECA. This gene encodes a kinase localized at the endoplasmic reticulum. This enzyme phosphorylates the alpha subunit of EIF2 in the unfolded protein response pathway, leading to inhibition of the translation. Also known as *PERK*, this protein has been involved in normal intestinal epithelial stem cell differentiation under homeostatic conditions [33]. Levels of *PPFIBP2* are twice lower in I-ECA than in G-ECA (Figure 5). Also known as *liprin-β2*, this gene encodes a protein member of the LAR family involved in axon guidance and neuronal synapse development [34]. Recently high levels of expression have been negatively associated with breast tumor cell motility and invasion by inhibiting the degradation of the extracellular matrix [35].

In conclusion, we identified a distinct molecular profile for the three most frequent categories of ECA, distinguishing U-ECA from G-ECA and I-ECA. Although, both U-ECA and I-ECA are HPV-related, they have a different molecular pattern justifying their diagnosis as separate entities.

Financial support: Lyon University Hospital (Hospices Civils de Lyon)

Author contributions: Damien Vasseur: Formal analysis, Data curation, Writing original draft; Jonathan Lopez: Conceptualization, Data curation, Methodology, Project administration, Supervision, Validation, Writing review & editing; Sabrina Croce: Data curation, Formal analysis, Resources, Writing review & editing; Garance Tondeur: Formal analysis, Writing original draft; Lucie Bonin: Resources; Françoise Descotes: Data curation, Supervision, Writing review and editing; François Golfier: Resources, Writing review and editing; Mojgan Devouassoux-Shisheboran: Conceptualization, Data curation, Formal analysis, Resources, Writing review & editing, Funding.

Declaration of competing interest: None

Acknowledgments

References

- [1] Kojima A, Mikami Y, Sudo T, Yamaguchi S, Kusanagi Y, Ito M, et al. Gastric Morphology and Immunophenotype Predict Poor Outcome in Mucinous Adenocarcinoma of the Uterine Cervix: The American Journal of Surgical Pathology 2007;31:664–72. <https://doi.org/10.1097/01.pas.0000213434.91868.b0>.
- [2] Kurman RJ, Carcangiu ML, Herrington CS, Young RH. WHO classification of tumours of female reproductive organs. 4th ed. Lyon: International Agency for Research on Cancer; 2014.
- [3] Stolnicu S, Barsan I, Hoang L, Patel P, Terinte C, Pesci A, et al. International Endocervical Adenocarcinoma Criteria and Classification (IECC): A New Pathogenetic Classification for Invasive Adenocarcinomas of the Endocervix. The American Journal of Surgical Pathology 2018;42:214–26. <https://doi.org/10.1097/PAS.0000000000000986>.
- [4] Pirog EC, Park KJ, Kiyokawa T, Zhang X, Chen W, Jenkins D, et al. Gastric-type Adenocarcinoma of the Cervix: Tumor With Wide Range of Histologic Appearances. Adv Anat Pathol 2019;26:1–12. <https://doi.org/10.1097/PAP.0000000000000216>.
- [5] Carleton C, Hoang L, Sah S, Kiyokawa T, Karamurzin YS, Talia KL, et al. A Detailed Immunohistochemical Analysis of a Large Series of Cervical and Vaginal Gastric-type Adenocarcinomas: The American Journal of Surgical Pathology 2016;40:636–44. <https://doi.org/10.1097/PAS.0000000000000578>.
- [6] Nucci MR, Clement PB, Young RH. Lobular endocervical glandular hyperplasia, not otherwise specified: a clinicopathologic analysis of thirteen cases of a distinctive pseudoneoplastic lesion and comparison with fourteen cases of adenoma malignum. Am J Surg Pathol 1999;23:886–91.
- [7] Kuragaki C, Enomoto T, Ueno Y, Sun H, Fujita M, Nakashima R, et al. Mutations in the STK11 gene characterize minimal deviation adenocarcinoma of the uterine cervix. Lab Invest 2003;83:35–45.
- [8] Garg S, Nagaria TS, Clarke B, Freedman O, Khan Z, Schwock J, et al. Molecular characterization of gastric-type endocervical adenocarcinoma using next-generation sequencing. Mod Pathol 2019. <https://doi.org/10.1038/s41379-019-0305-x>.
- [9] Köbel M, Piskorz AM, Lee S, Lui S, LePage C, Marass F, et al. Optimized p53 immunohistochemistry is an accurate predictor of TP53 mutation in ovarian carcinoma: p53 immunohistochemistry predicts TP53 mutation status. The Journal of Pathology: Clinical Research 2016;2:247–58. <https://doi.org/10.1002/cjp2.53>.
- [10] Köbel M, Luo L, Grevers X, Lee S, Brooks-Wilson A, Gilks CB, et al. Ovarian Carcinoma Histotype: Strengths and Limitations of Integrating Morphology With Immunohistochemical Predictions. International Journal of Gynecological Pathology 2019;38:353–62. <https://doi.org/10.1097/PGP.0000000000000530>.
- [11] Karamurzin YS, Kiyokawa T, Parkash V, Jotwani AR, Patel P, Pike MC, et al. Gastric-type Endocervical Adenocarcinoma: An Aggressive Tumor With Unusual Metastatic Patterns and Poor Prognosis. The American Journal of Surgical Pathology 2015;39:1449–57. <https://doi.org/10.1097/PAS.0000000000000532>.
- [12] Martinez I, Wang J, Hobson KF, Ferris RL, Khan SA. Identification of differentially expressed genes in HPV-positive and HPV-negative oropharyngeal squamous cell carcinomas. European Journal of Cancer 2007;43:415–32. <https://doi.org/10.1016/j.ejca.2006.09.001>.
- [13] Vaishnavi A, Capelletti M, Le AT, Kako S, Butaney M, Ercan D, et al. Oncogenic and drug-sensitive NTRK1 rearrangements in lung cancer. Nature Medicine 2013;19:1469–72. <https://doi.org/10.1038/nm.3352>.

- [14] Greco A, Miranda C, Pierotti MA. Rearrangements of NTRK1 gene in papillary thyroid carcinoma. *Molecular and Cellular Endocrinology* 2010;321:44–9. <https://doi.org/10.1016/j.mce.2009.10.009>.
- [15] Martin, Tracey, Mansel R, Jiang W. Loss of occludin leads to the progression of human breast cancer. *International Journal of Molecular Medicine* 2010;26. https://doi.org/10.3892/ijmm_00000519.
- [16] Osanai M, Murata M, Nishikiori N, Chiba H, Kojima T, Sawada N. Epigenetic Silencing of Occludin Promotes Tumorigenic and Metastatic Properties of Cancer Cells via Modulations of Unique Sets of Apoptosis-Associated Genes. *Cancer Research* 2006;66:9125–33. <https://doi.org/10.1158/0008-5472.CAN-06-1864>.
- [17] Förster S, Gretschel S, Jöns T, Yashiro M, Kemmner W. THBS4, a novel stromal molecule of diffuse-type gastric adenocarcinomas, identified by transcriptome-wide expression profiling. *Modern Pathology* 2011;24:1390–403. <https://doi.org/10.1038/modpathol.2011.99>.
- [18] Greco SA, Chia J, Inglis KJ, Cozzi S-J, Ramsnes I, Buttenshaw RL, et al. Thrombospondin-4 is a putative tumour-suppressor gene in colorectal cancer that exhibits age-related methylation. *BMC Cancer* 2010;10. <https://doi.org/10.1186/1471-2407-10-494>.
- [19] Dakhova O, Ozen M, Creighton CJ, Li R, Ayala G, Rowley D, et al. Global Gene Expression Analysis of Reactive Stroma in Prostate Cancer. *Clinical Cancer Research* 2009;15:3979–89. <https://doi.org/10.1158/1078-0432.CCR-08-1899>.
- [20] McCart Reed AE, Song S, Kutasovic JR, Reid LE, Valle JM, Vargas AC, et al. Thrombospondin-4 expression is activated during the stromal response to invasive breast cancer. *Virchows Archiv* 2013;463:535–45. <https://doi.org/10.1007/s00428-013-1468-3>.
- [21] Liu Y, Deng J, Wang L, Lee H, Armstrong B, Scuto A, et al. S1PR1 is an effective target to block STAT3 signaling in activated B cell-like diffuse large B-cell lymphoma. *Blood* 2012;120:1458–65. <https://doi.org/10.1182/blood-2011-12-399030>.
- [22] Ogretmen B. Sphingolipid metabolism in cancer signalling and therapy. *Nature Reviews Cancer* 2018;18:33–50. <https://doi.org/10.1038/nrc.2017.96>.
- [23] Chae S-S, Paik J-H, Furneaux H, Hla T. Requirement for sphingosine 1-phosphate receptor-1 in tumor angiogenesis demonstrated by in vivo RNA interference. *Journal of Clinical Investigation* 2004;114:1082–9. <https://doi.org/10.1172/JCI200422716>.
- [24] Nie D, Guo Y, Yang D, Tang Y, Chen Y, Wang M-T, et al. Thromboxane A2 Receptors in Prostate Carcinoma: Expression and Its Role in Regulating Cell Motility via Small GTPase Rho. *Cancer Research* 2008;68:115–21. <https://doi.org/10.1158/0008-5472.CAN-07-1018>.
- [25] Watkins G, Douglas-Jones A, Mansel RE, Jiang WG. Expression of thromboxane synthase, TBXAS1 and the thromboxane A2 receptor, TBXA2R, in human breast cancer. *Int Semin Surg Oncol* 2005;2:23. <https://doi.org/10.1186/1477-7800-2-23>.
- [26] Li X, Tai H-H. Activation of thromboxane A2 receptors induces orphan nuclear receptor Nurr1 expression and stimulates cell proliferation in human lung cancer cells. *Carcinogenesis* 2009;30:1606–13. <https://doi.org/10.1093/carcin/bgp161>.
- [27] Lee J-H, Miele ME, Hicks DJ, Phillips KK, Trent JM, Weissman BE, et al. KiSS-1, a Novel Human Malignant Melanoma Metastasis-Suppressor Gene. *JNCI Journal of the National Cancer Institute* 1996;88:1731–7. <https://doi.org/10.1093/jnci/88.23.1731>.
- [28] Sanchez-Carbayo M, Capodiecì P, Cordon-Cardo C. Tumor Suppressor Role of KiSS-1 in Bladder Cancer. *The American Journal of Pathology* 2003;162:609–17. [https://doi.org/10.1016/S0002-9440\(10\)63854-0](https://doi.org/10.1016/S0002-9440(10)63854-0).

- [29] Lee J-H, Welch DR. Suppression of Metastasis in Human Breast Carcinoma MDA-MB-435 Cells after Transfection with the Metastasis Suppressor Gene, *KiSS-1*. *Cancer Res* 1997;57:2384.
- [30] Zheng S, Chang Y, Hodges KB, Sun Y, Ma X, Xue Y, et al. Expression of KISS1 and MMP-9 in non-small cell lung cancer and their relations to metastasis and survival. *Anticancer Res* 2010;30:713–8.
- [31] Martin TA, Watkins G, Jiang WG. KiSS-1 Expression in Human Breast Cancer. *Clinical & Experimental Metastasis* 2005;22:503–11. <https://doi.org/10.1007/s10585-005-4180-0>.
- [32] Savvidis C, Papaiconomou E, Petraki C, Msaouel P, Koutsilieris M. The role of KISS1/KISS1R system in tumor growth and invasion of differentiated thyroid cancer. *Anticancer Res* 2015;35:819–26.
- [33] Heijmans J, van Lidth de Jeude JF, Koo B-K, Rosekrans SL, Wielenga MCB, van de Wetering M, et al. ER Stress Causes Rapid Loss of Intestinal Epithelial Stemness through Activation of the Unfolded Protein Response. *Cell Reports* 2013;3:1128–39. <https://doi.org/10.1016/j.celrep.2013.02.031>.
- [34] Serra-Pagès C, Medley QG, Tang M, Hart A, Streuli M. Liprins, a Family of LAR Transmembrane Protein-tyrosine Phosphatase-interacting Proteins. *Journal of Biological Chemistry* 1998;273:15611–20. <https://doi.org/10.1074/jbc.273.25.15611>.
- [35] Chiaretti S, Astro V, Chiricozzi E, Curtis I de. Effects of the scaffold proteins liprin- α 1, β 1 and β 2 on invasion by breast cancer cells. *Biology of the Cell* 2016;108:65–75. <https://doi.org/10.1111/boc.201500063>.

Figure legends

Figure 1: Hematoxylin and Eosin (H&E) Staining of the three groups of endocervical adenocarcinomas, 100x magnification. A. Mucinous gastric-type ECA composed of fused glands, characterized by abundant pale cytoplasm and distinct cell borders. B. Mucinous intestinal-type ECA composed of glands lined by columnar goblet cells with pools of mucin dissecting the cervical stroma. C. Usual-type ECA composed of closely packed glands lined by stratified columnar cells with numerous mitoses and apoptotic bodies and diminished mucin secretion.

Figure 2: Gene-expression signature to distinguish usual-type from mucinous carcinomas. A. Heatmap built using a 9-genes signature to compare U-ECA to mucinous ECA. U-ECA cases cluster on the left part of the figure whereas I-ECA and G-ECA cases are mixed on the right part. On top of the figure HPV, Muc6, p53 and p16 status are detailed for each sample. B. Distance matrix, other representation of the dichotomy of the samples. Blue stands for an absence of distance between samples (highly similar) whereas orange stands for high distances between them.

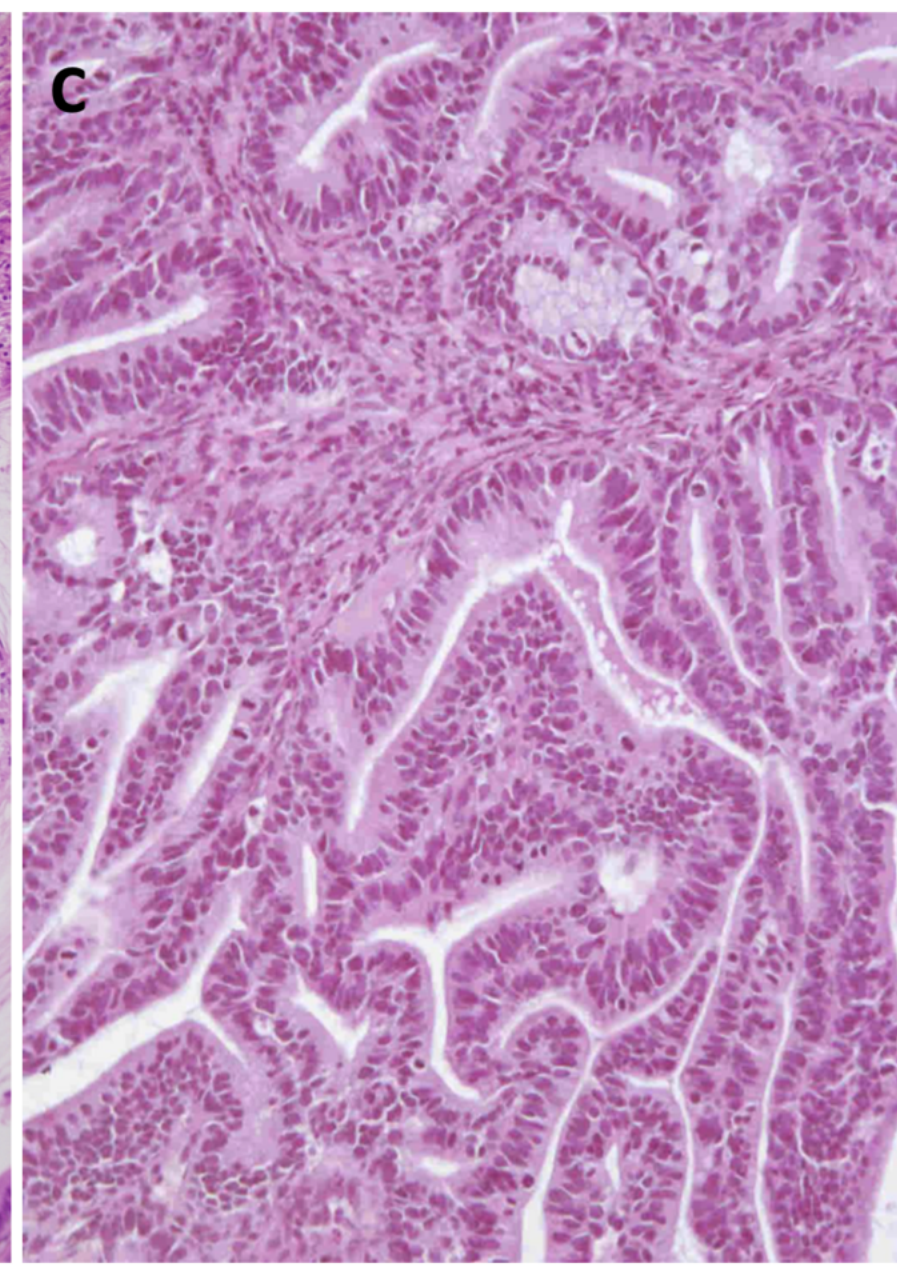
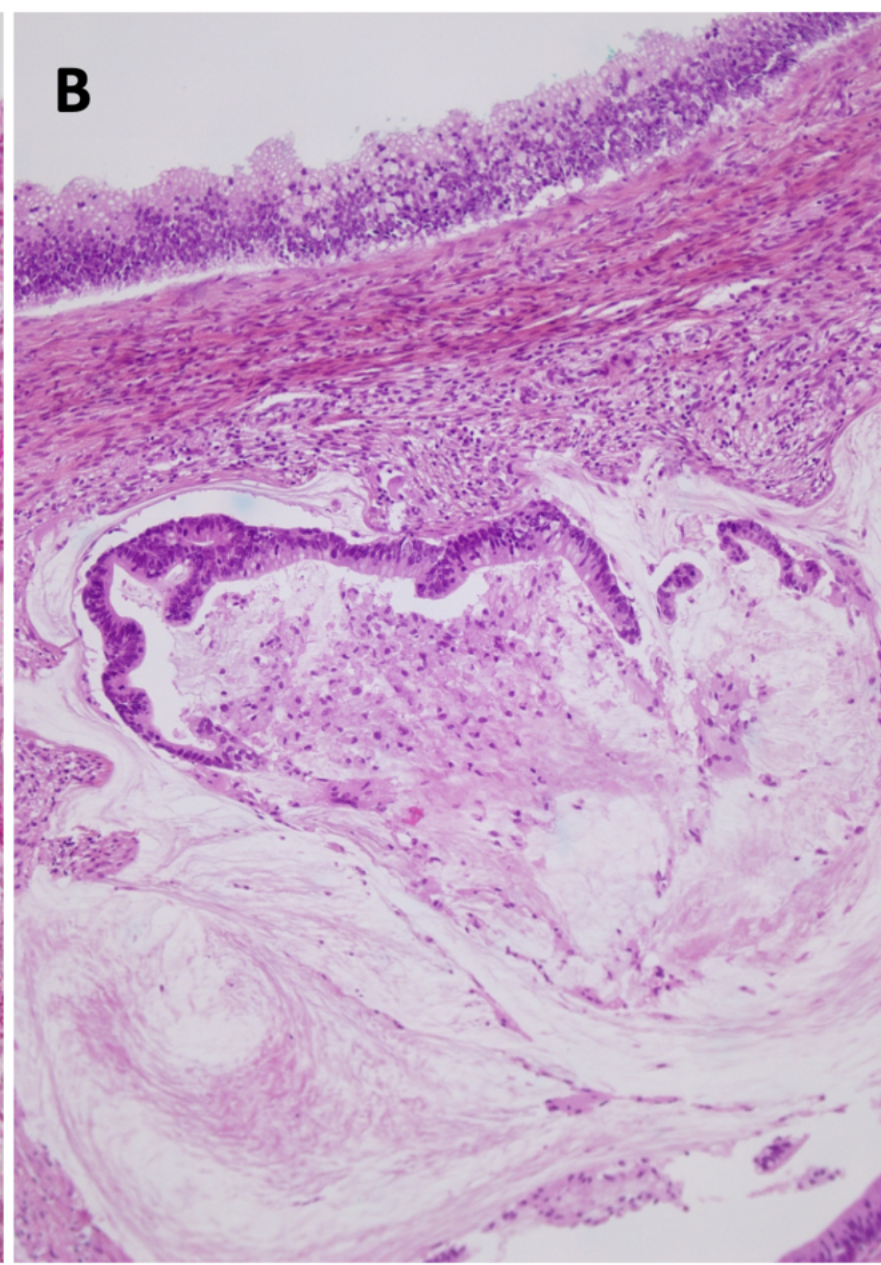
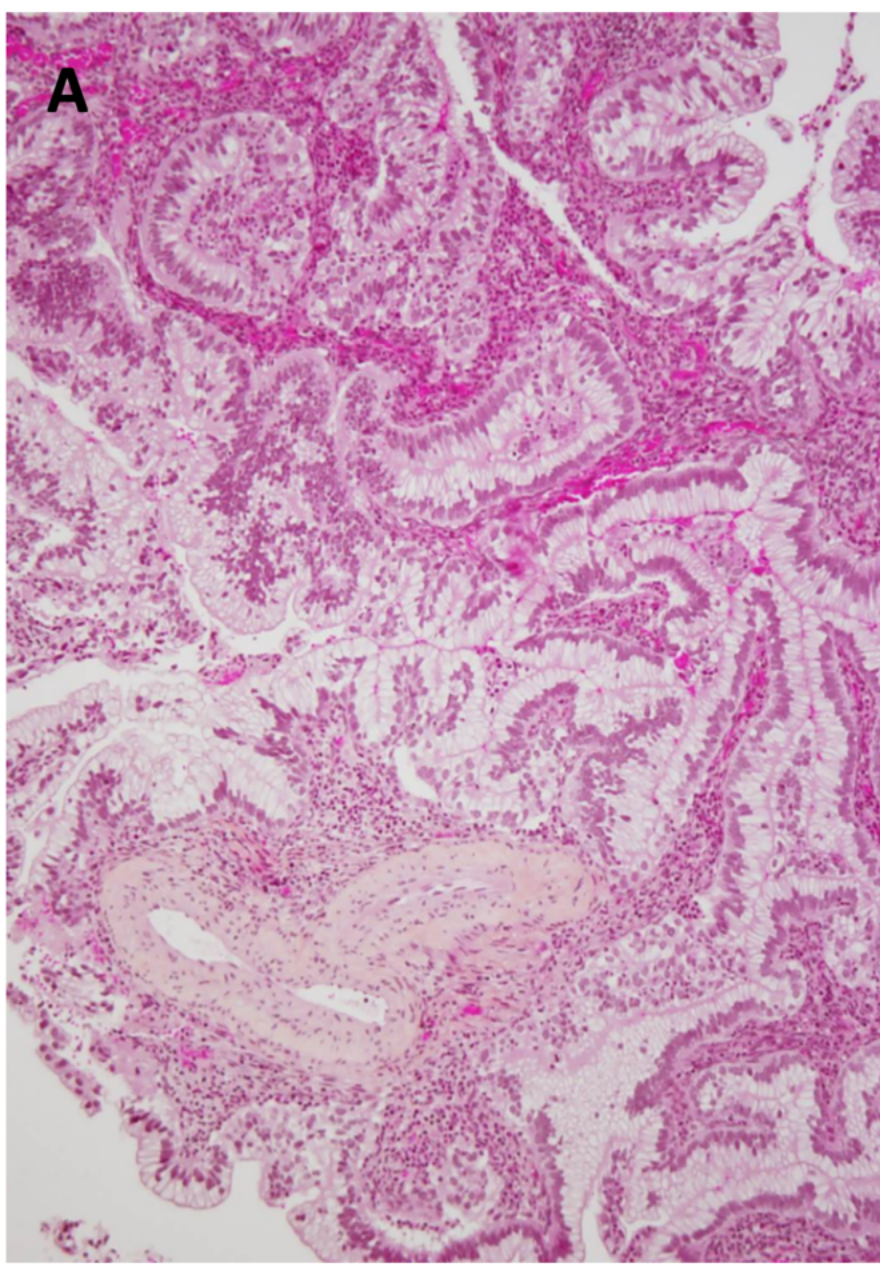
Figure 3: Immunohistochemical study of occludin (A and C) and claudin 4 (B and D) in gastric-type and usual type endocervical ECA. A. Low membranous expression of OCLN (200X). B. Loss of claudin 4 in a representative G-ECA (200X). C. High membranous expression of occludin in a representative U-ECA (100X). D. High membranous expression of claudin 4 in a representative U-ECA (100X).

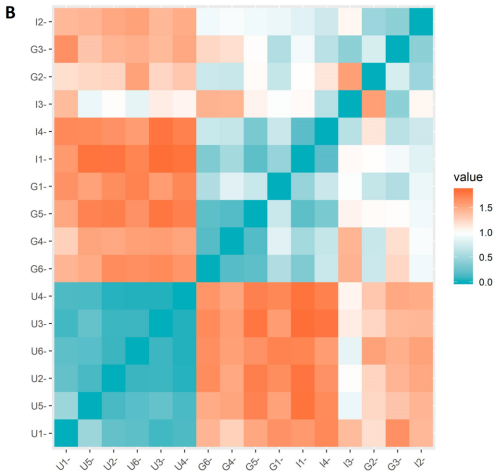
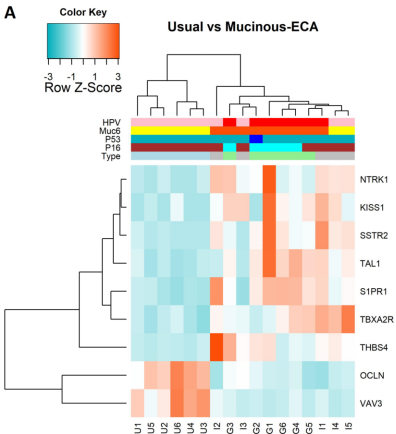
Figure 4: Molecular differences between gastric and intestinal types. A. Heatmap based on an 11-genes signature. On the left part of the figure, G-ECA are clustering together. They are characterized by high levels of PPFIBP2, DENND5A, ASPN, GATA4, VEGFB and ZFYVE16. On the right side are localized I-ECA with high levels of HSP90B1, AKT1, RPS6KB2, EIF2AK3 and

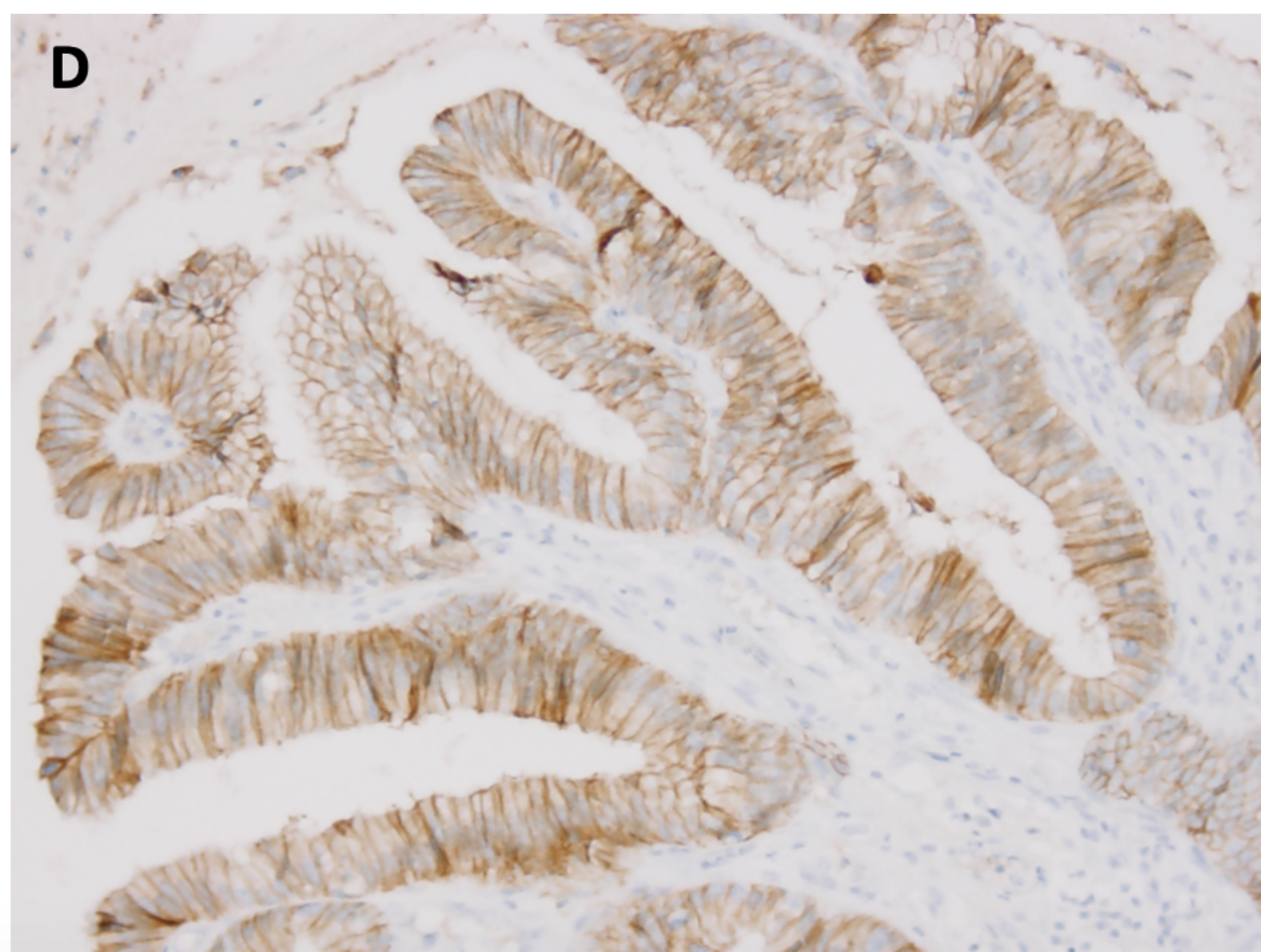
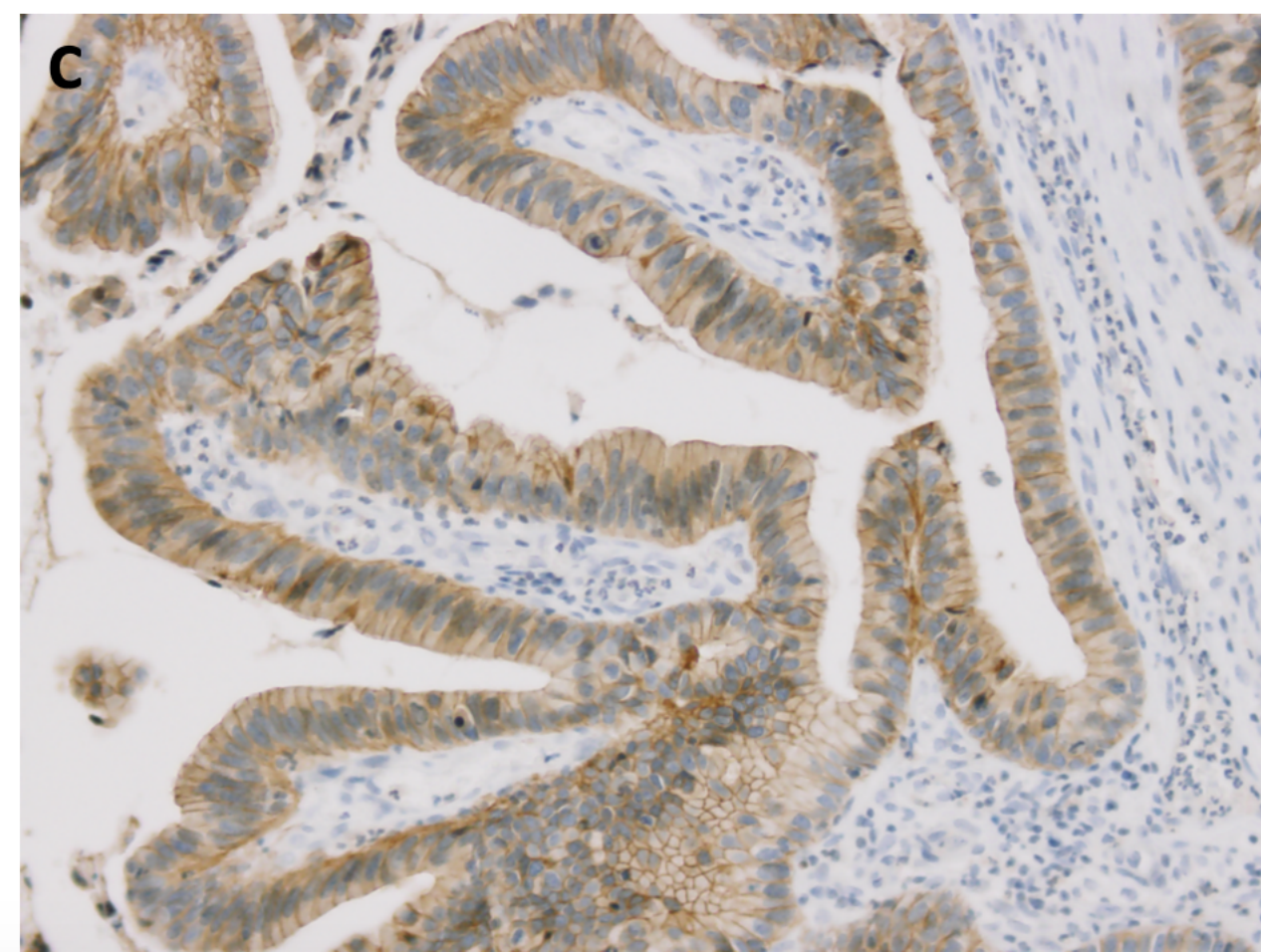
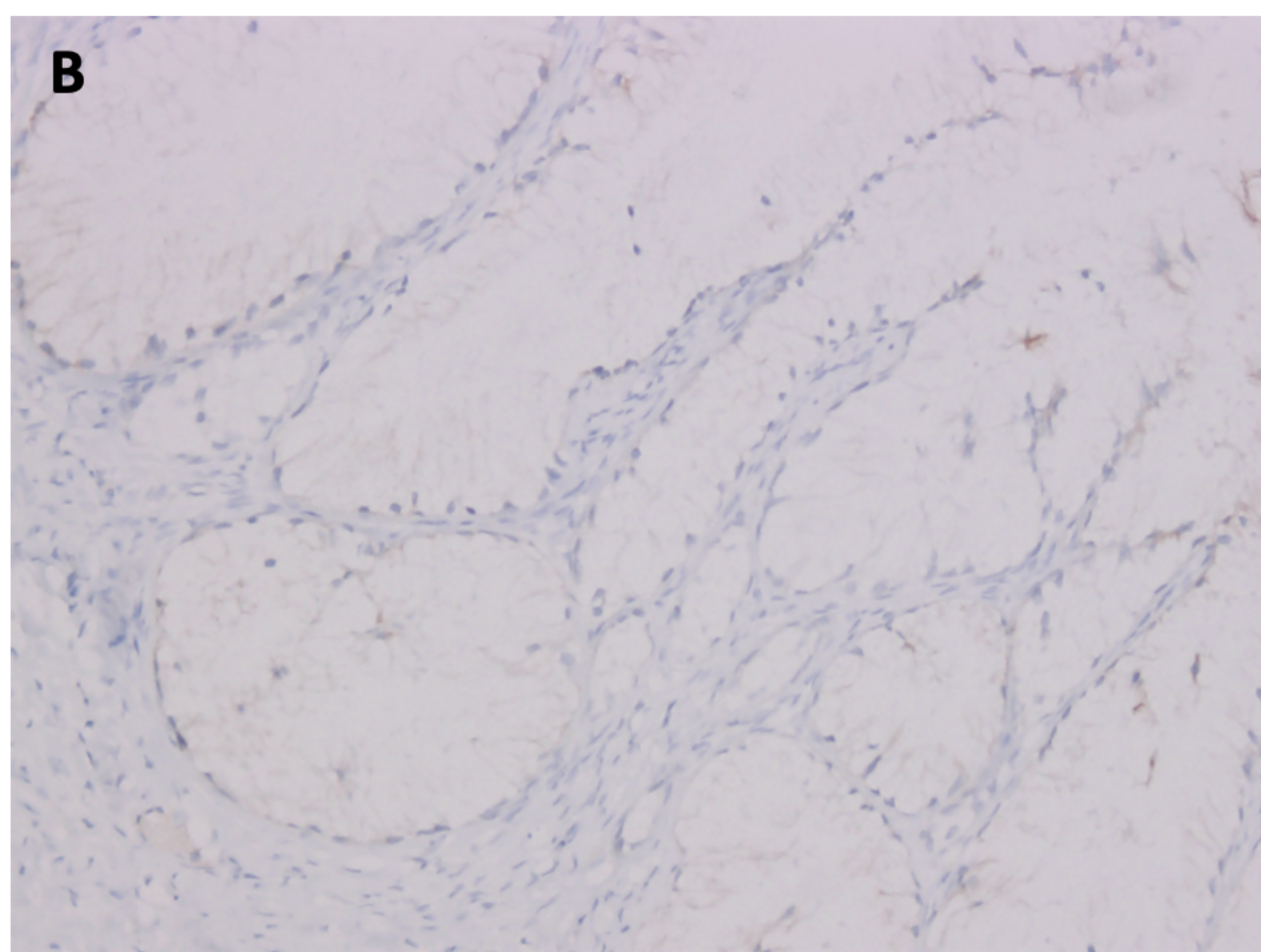
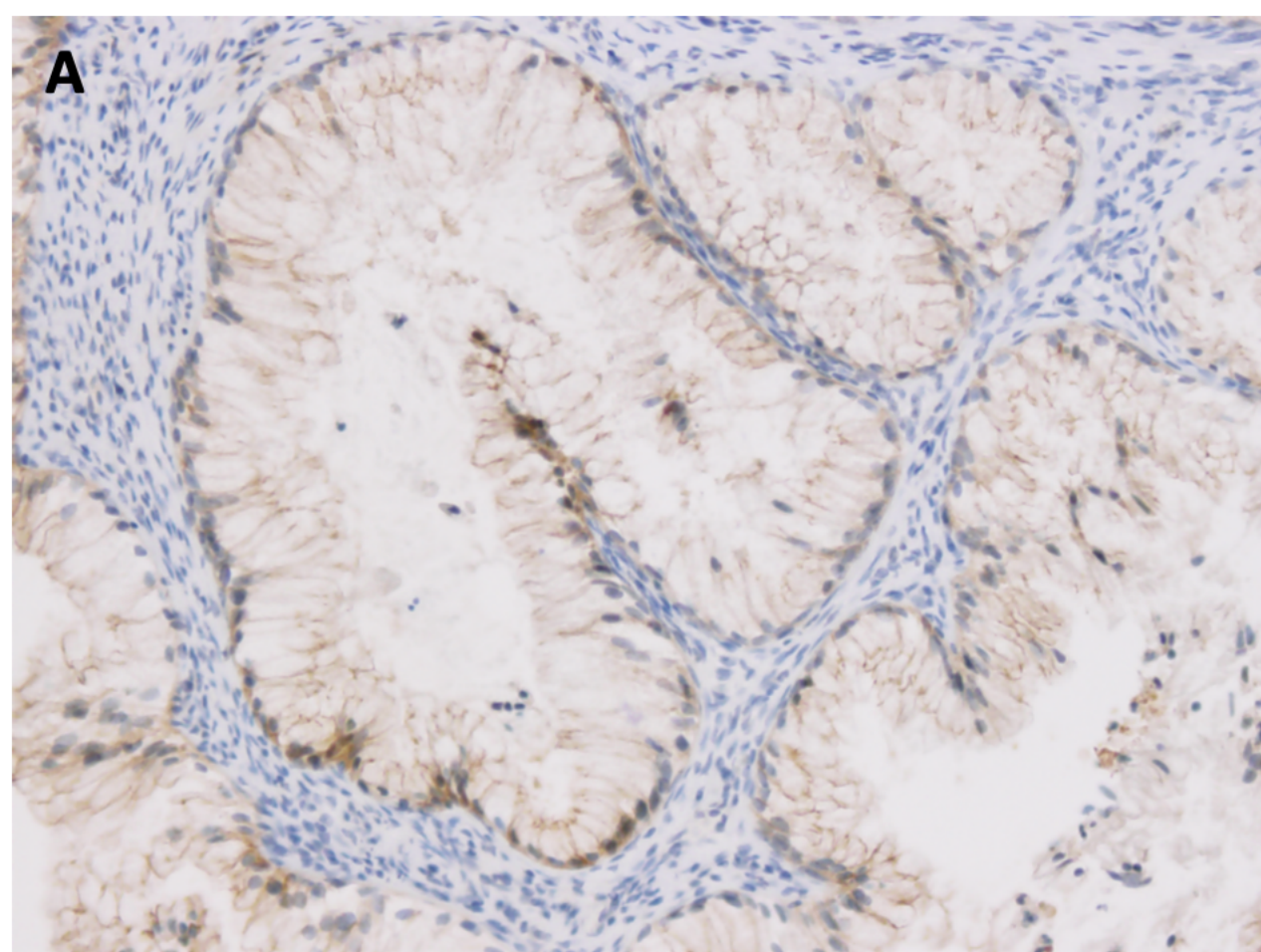
PTTG1. B. String network of the second signature. 6 of the 11 genes are involved in the AKT pathway.

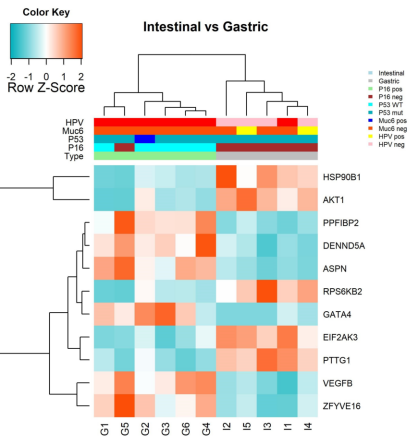
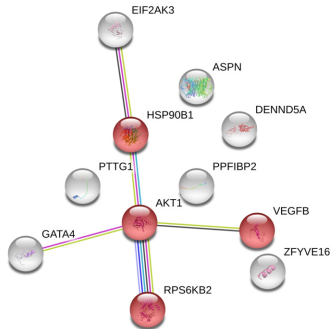
Figure 5: Composite gene expression signature to classify usual-, intestinal- and gastric-type ECA. A. Heatmap of the 11 selected genes. U-ECA clustered on the left, I-ECA in the middle and G-ECA on the right. B. Principal Component Analysis. Red dots represent the individual samples. Green arrows are vectors for the different genes.

Figure 6: Correlation matrix. Orange's dots are for strong positive correlation, whereas light blue's dots are for a strong negative correlation. A black cross indicates a non-significant correlation taking a risk $\alpha=0.05$.







A**B**

PCA - Biplot

